

# Drive-by-wireless for Vehicle Control and Monitor using Wireless Controller Area Network (WCAN)

S.Srinath

B. Tech Student, School of Electronics Engineering  
Vellore Institute of Technology  
Vellore, India  
srinath.s2011@vit.ac.in

Gerardine Immaculate Mary

Assistant Professor (Selection Grade)  
Vellore Institute of Technology  
Vellore, India  
gerardine@vit.ac.in

**Abstract**—Wired systems are complex, heavy, less secure and expensive. Hence, in today's 21<sup>st</sup> century wireless technology has been gradually adopted by automobile manufacturers. A vehicle has various control units which were connected using traditional point-to-point wiring architecture in olden days. These were replaced by a CAN bus later. This paper uses Wireless CAN (WCAN) to interconnect various control units. This has several important advantages such as system flexibility, message routing, filtering, multicast, together with data consistency. This paper proposes a drive-by-wireless technique for vehicle control and monitor functions using Wireless Controller Area Network. Traditional hydraulic or mechanical methods of steering, braking and accelerating of a vehicle will be replaced by Drive by Wireless Technique. Also, traditional vehicle monitoring methods are done in a wireless manner. The algorithm includes Unique Identification Codes which is sent with all the transactions involving wireless communication packets to reduce interference from adjacent drive-by-wireless system.

**Keywords**- Drive-by-wireless; WCAN; Vehicle Control and Monitor; Unique Identification Codes

## I. INTRODUCTION

Drive-by-wireless techniques replace the mechanical and hydraulic connections between the driver and the associated vehicle actuators with electronic communication systems. These systems transmit electronic messages to direct a vehicle component based on the action taken by the driver of the vehicle, e.g., turning a steering wheel, pressing a brake pedal, or pressing an accelerator pedal [1]. In the past the vehicle bus communication used point to point communication wiring systems which causes complexity, bulkiness, is expensive with increasing electronics and controller deployed vehicles. The abundance of wiring required makes the whole circuit complicated. CAN solves this complexity by using twisted pair cables that is shared throughout the control. Not only does it reduce the wiring complexity but it also made it possible to interconnect several devices using only single pair of wires and allowing them to have simultaneous data exchange. WCAN has several important advantages such as system flexibility, message routing, filtering, multicast, together with data consistency [2]. The new WCAN is proposed to

exploit the advantages of CAN and still providing wireless access. The rest of the paper is organized as follows; section II outlines the related work and Drive-by-wireless technique, section III describes the block diagram of the system, section IV briefs on the components used, section V presents the circuit diagram of the system, section VI discusses algorithm, section VII presents the hardware output and section VIII briefs the conclusion.

## II. RELATED WORK AND DRIVE-BY-WIRELESS TECHNIQUE

Stähle et. Al [1] investigated the so-called drive-by-wireless, i.e., using a wireless network to control steering, braking, accelerating and other functions within an automobile. Mary et.al [2] showed that WCAN is suited for real time control applications giving maximum throughput for minimal latency for an optimized number of nodes. Iturri et. Al [11] showed that ZigBee is a viable technology for successfully deploying intra-car wireless sensor networks. Lin et. Al [3] proposed an Intra-car Wireless Sensor Network (WSN) to eliminate the amount of wiring harness and simplify the wiring structure. Lin et. Al [6] evaluated the performance of intra-vehicular wireless sensor networks (IVWSNs) under interference from WiFi and Bluetooth devices. Torbitt et. Al [7] analyzed the surface wave hypothesis at different frequencies in intra-vehicular environments. Ahmed et. Al [8] investigated the issues around replacing the current wired data links between electrical control units (ECU) and sensors/switches in a vehicle, with wireless links. Lin et. Al [9] proposed a new wireless technology known as Bluetooth Low Energy (BLE) and outlined a new architecture for IVWSN. This paper proposes Drive-by-wireless technique using WCAN.

### A. Drive-by-wire System

Drive-by-wire technology in the automotive industry is the use of electrical or electro-mechanical systems for performing vehicle functions traditionally achieved by mechanical linkages. This technology replaces the traditional mechanical control systems with electronic control systems using electromechanical actuators and human-machine interfaces such as pedal and steering feel emulators. The Drive-by-wire system used point to point

communication wiring systems as shown in Figure 1. This causes complexity, heaviness and is expensive.

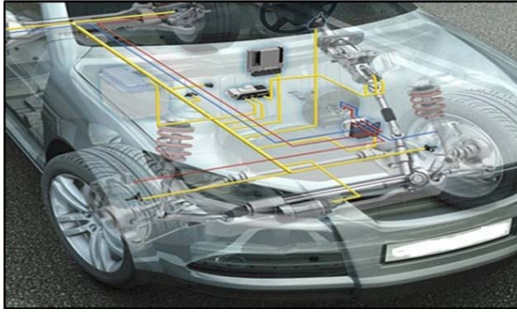


Figure 1. Existing System

### B. Drive-by-wireless System

The Drive-by-wireless system ensures less weight, safety and comfort. The position of the sensor, motor and the wheel for the proposed Drive-by-wireless system is shown in Figure 2.

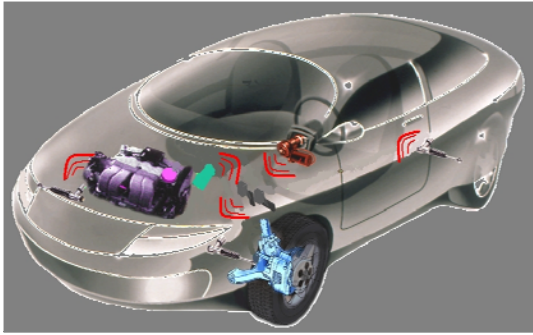


Figure 2. Drive-by-wireless System

### III. BLOCK DIAGRAM OF THE PROPOSED SYSTEM

The block diagram of the system is presented in Figure 3. The system has four microcontroller units and ZigBee over 802.15.4 protocol is used for wireless communication.

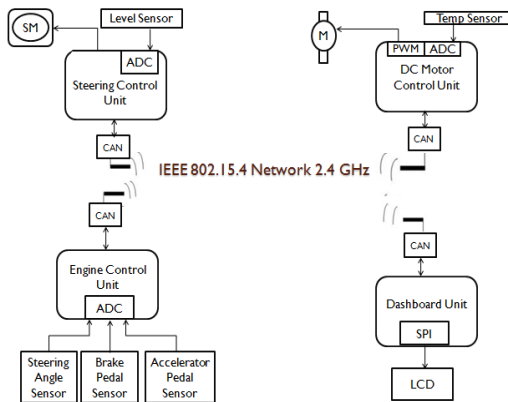


Figure 3. Block Diagram

The Steering, Brake, Accelerator sensors are associated with the Engine Control Unit. The Dashboard

unit contains the LCD, the D.C. Motor unit contains a D.C. motor with a motor drive and a temperature sensor. Finally, the Servo Motor Unit contains a Servo Motor and a level sensor.

### IV. COMPONENTS DESCRIPTION

PIC18F45K22 is the microcontroller used in the project. Circular potentiometers are used for Brake-Acceleration and Steering. Servo Motor and a level sensor is used for the Servo Motor Unit and DC Motor unit contains a D.C. motor with a motor drive and a temperature sensor. LCD Display is used for displaying the engine temperature and fuel levels.

#### A. PIC18F45K22

PIC18(L)F45K22 has 32k program memory, 1536 bytes of SRAM and 256bytes of EEPROM. It has three 8-bit timers and four 16-bit timers. All of the devices in the PIC18(L)F2X/4XK22 family offer ten different oscillator options, allowing users a wide range of choices in developing application hardware. These include:

- Four Crystal modes, using crystals or ceramic resonators
- Two External Clock modes, offering the option of using two pins (oscillator input and a divide-by-4 clock output) or one pin (oscillator input, with the second pin reassigned as general I/O)
- Two External RC Oscillator modes with the same pin options as the External Clock modes
- An internal oscillator block which contains a 16 MHz HFINTOSC oscillator and a 31 kHz LFINTOSC oscillator, which together provide eight user selectable clock frequencies, from 31 kHz to 16 MHz. This option frees the two oscillator pins for use as additional general purpose I/O.
- A Phase Lock Loop (PLL) frequency multiplier, available to both external and internal oscillator modes, which allows clock speeds of up to 64 MHz. Used with the internal oscillator, the PLL gives users a complete selection of clock speeds, from 31 kHz to 64 MHz – all without using an external crystal or clock circuit.

40-pin PDIP

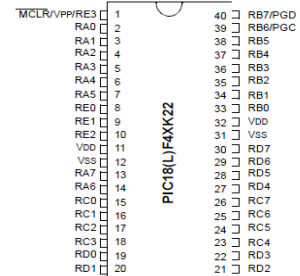


Figure 4. PIC18F45K22 Microcontroller

#### B. Potentiometers

A potentiometer is a three terminal resistor with a sliding contact forms an adjustable voltage divider and only two terminals are used one end and the wiper acts as a variable resistor or rheostat. Electric potential is measured by potentiometer device.

### C. LCD Display

The HD44780U dot-matrix liquid crystal display controller and driver LSI displays alphanumeric, Japanese kana characters, and symbols. It can be configured to drive a dot-matrix liquid crystal display under the control of a 4- or 8-bit microprocessor. Since all the functions such as display RAM, character generator, and liquid crystal driver, required for driving a dot-matrix liquid crystal display are internally provided on one chip, a minimal system can be interfaced with this controller/driver. A single HD44780U can display up to one 8-character line or two 8-character lines. The HD44780U has pin function compatibility with the HD44780S which allows the user to easily replace an LCD-II with an HD44780U. The HD44780U character generator ROM is extended to generate 208 5x8 dot character fonts and 32 5 x10 dot character fonts for a total of 240 different character fonts. The low power supply (2.7V to 5.5V) of the HD44780U is suitable for any portable battery-driven product requiring low power dissipation.

### D. DC Motor

A DC motor has a two wire connection. All drive power is supplied over these wires. Most DC motors are pretty fast of about 5000 rpm. The DC motor speed is controlled by a technique called pulse width modulation or PWM.



Figure 5. D.C. Motor

### E. Servo Motor

The function of the servo is to receive a control signal that represents a desired output position of the servo shaft, and apply power to its DC motor until the shaft turns to that position. It uses position sensing device to rotate the shaft. The shaft can turn a maximum of 200 degree so back and forth.



Figure 6. Servo Motor

### F. Pressure Sensor

The MPX5010/MPXV5010G series piezoresistive transducers are state-of-the-art monolithic silicon pressure sensors designed for a wide range of applications, but

particularly those employing a microcontroller or microprocessor with A/D inputs. This transducer combines advanced micromachining techniques, thin-film metallization, and bipolar processing to provide an accurate, high level analog output signal that is proportional to the applied pressure.

It's features are

- . 5.0% Maximum Error over 0° to 85°C
- . Ideally Suited for Microprocessor or Microcontroller-Based Systems
- . Durable Epoxy Unibody and Thermoplastic (PPS) Surface Mount Package
- . Temperature Compensated over .40° to +125°C



Figure 7. Pressure Sensor

### G. Temperature Sensor

The LM35 series are precision integrated-circuit temperature sensors, whose output voltage is linearly proportional to the Celsius (Centigrade) temperature. The LM35 thus has an advantage over linear temperature sensors calibrated in ° Kelvin, as the user is not required to subtract a large constant voltage from its output to obtain convenient Centigrade scaling. The LM35 does not require any external calibration or trimming to provide typical accuracies of  $\pm 1/4^\circ\text{C}$  at room temperature and  $\pm 3/4^\circ\text{C}$  over a full  $-55$  to  $+150^\circ\text{C}$  temperature range. Low cost is assured by trimming and calibration at the wafer level. The LM35's low output impedance, linear output, and precise inherent calibration make interfacing to readout or control circuitry especially easy. It can be used with single power supplies, or with plus and minus supplies. As it draws only 60  $\mu\text{A}$  from its supply, it has very low self-heating, less than  $0.1^\circ\text{C}$  in still air. The LM35 is rated to operate over a  $-55^\circ$  to  $+150^\circ\text{C}$  temperature range, while the LM35C is rated for a  $-40^\circ$  to  $+110^\circ\text{C}$  range ( $-10^\circ$  with improved accuracy). The LM35 series is available packaged in hermetic TO-46 transistor packages, while the LM35C, LM35CA, and LM35D are also available in the plastic TO-92 transistor package. The LM35D is also available in an 8-lead surface mount small outline package and a plastic TO-220 package.

### H. CAN MCP2515

It is a Stand-Alone CAN Controller with SPI Interface, 18 pin I.C.

- Implements CAN V2.0B at 1 Mb/s: 0 – 8 byte length in the data field, Standard and extended data and remote frames
- Receive Buffers, Masks and Filters:  
Two receive buffers with prioritized message Storage, Six 29-bit filters and Two 29-bit masks

- Data Byte Filtering on the First Two Data Bytes (applies to standard data frames)
- Three Transmit Buffers with Prioritization and Abort Features
- High-Speed SPI Interface (10 MHz): SPI modes 0,0 and 1,1
- One-Shot mode Ensures Message Transmission is Attempted Only One Time
- Clock Out Pin with Programmable Prescaler: Can be used as a clock source for other device(s)
- Start-of-Frame Signal is Available for Monitoring the SOF Signal: Can be used for time-slot-based protocols and/or bus diagnostics to detect early bus degradation

## V. CIRCUIT DIAGRAM

The system comprises of four control units which communicate with each other using Zigbee over 802.15.4 protocol. The four modules are Engine Control Unit, D.C. Motor Unit, Servo Motor Unit and the Dashboard Unit.

The input 220V A.C. power supply is converted to 12V D.C. by an adapter. Various units in the modules require only 5V D.C and 3.3 V D.C. power supply. Hence a regulator is used for this purpose. The PIC18F45K22 microcontroller is a 40 pin I.C. There are 5 ports. Port A, B, C and D have 8 pins each while Port E has 3 pins. The remaining 5 pins are used for MCLR, VDD and Ground. The ICSP (In Circuit Serial Programmer) is a 5 pin device which is used by PitKit 3 to dump the program from the computer to the microcontroller. Pin 1 of the ICSP is connected to a high voltage to erase any previous programs, Pin 2 is the clock, Pin 3 is the data, Pin 4 is connected to Ground while Pin 5 is connected to VDD.

The Dashboard Module circuit diagram is shown in Figure 8. It consists of a 16x2 LCD display.

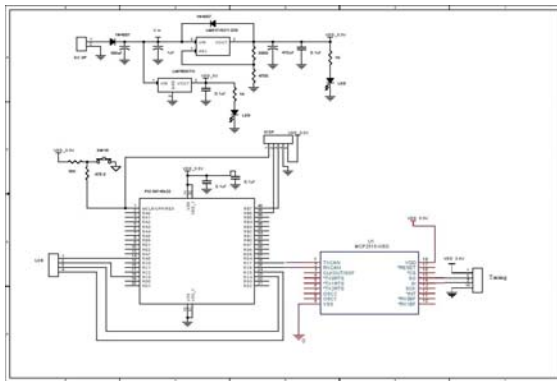


Figure 8. The Dashboard Module

SP1 and SP2 of the PIC18F45K22 are pins A5, C3, C4, C5 and A6, C3, C4, C5 respectively. A5 and A6 are the Enable Pin, C3 is the clock, C4 is the Data Input and C5 is the Data Output. UART1 and UART2 are pins 25, 26 and 29, 30 respectively. 25 and 29 are for transmission while 26 and 30 are for reception. In CAN, CANL is for transmission and CANH is for reception. In Zigbee Pin 2 is for transmission and Pin 3 is for reception.

As shown in Figure 9, Pin 1 of Port C is used for the motor drive circuit while Pin 1 of Port A is used for the pressure sensor.

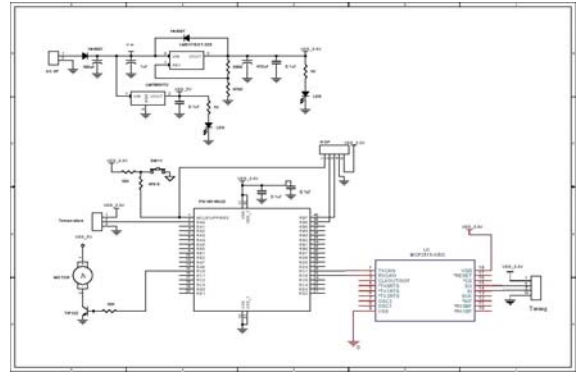


Figure 9. The D.C. Motor Module

As shown in Figure 10, Pin 1 of Port C is connected to the servo motor while Pin 1 of Port A is connected to the temperature sensor.

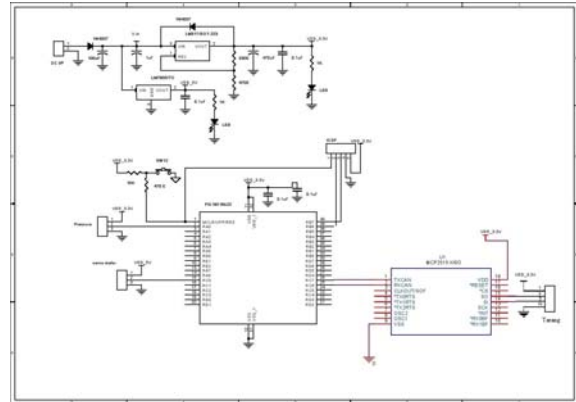


Figure 10. The Servo Motor Module

In Figure 11, the first three pins of Port A are connected to the Accelerator Sensor, Brake Sensor and Steering Sensor respectively.

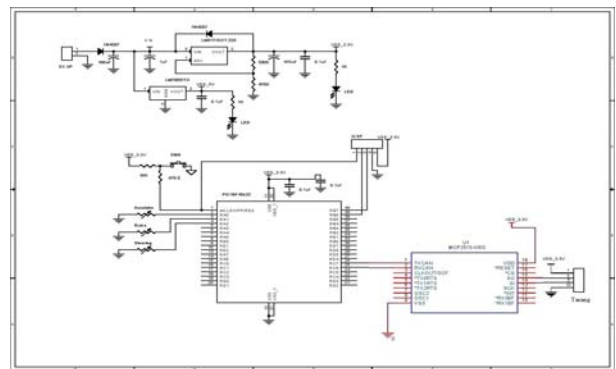


Figure 11. The Engine Control Module

## VI. ALGORITHM

Some of the pseudo-codes for various control units are shown below. MPLAB IDE is the development platform used for coding.

```

tostring(advalue1, dispstring);
cantx('A');

```

```

cantx(dispstring[0]);
cantx(dispstring[1]);
cantx(dispstring[2]);
cantx(dispstring[3]);
cantx(dispstring[4]);

```

In the above pseudo-code, the data obtained by various sensor units in the Engine Control Unit are converted into string and transmitted using CAN. Before transmission identification characteristics like 'A', 'B', etc are also transmitted.

```

if(adcvalue1 > adcvalue2)
    {
        accelerator = adcvalue1 - adcvalue2;
    }
else
    {
        accelerator = 0
    }

```

The above conditions are followed in the D.C. motor unit.

```

adcvalue1 = map(adcvalue1 , 0, 1023, 1, 150);
temp = adcvalue1;
angle1_act = temp;
angle11 = angle1_act/10;
datareceivedbit = 0;

```

The above condition is followed in the Servo motor unit. The ADC values obtained by the engine control module steering sensor is mapped as 1 for 0 and 150 for 1023 and the servo motor is driven.

## VII. HARDWARE OUTPUT

The Servo Motor Module is shown in Figure 12. It consists of a Servo Motor and a Level Sensor.

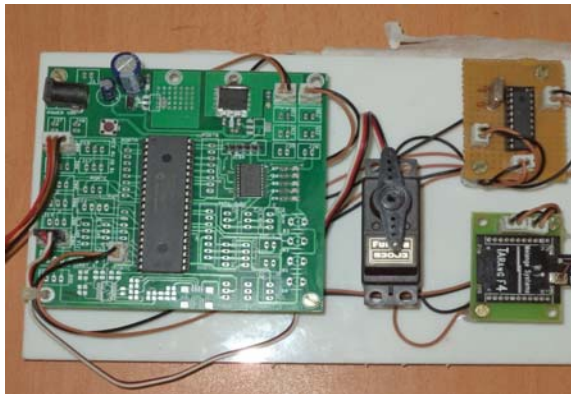


Figure 12. The Servo Motor Module

The Engine Control Module is shown in Figure 13. It consists of three sensors namely the accelerator sensor, the brake sensor and the steering sensor.



Figure 13. The Engine Control Module

The Dashboard Module is shown in Figure 14. It consists of a 16x2 LCD display.

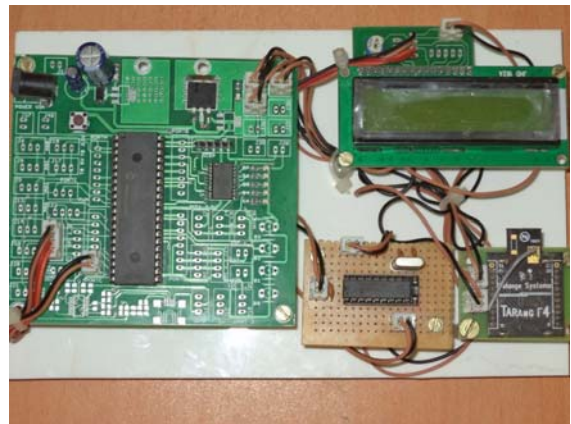


Figure 14. The Dashboard Module

The D.C. Motor Module is shown in Figure 15. It consists of a D.C. Motor and a Temperature Sensor.



Figure 15. The D.C. Motor Module

## VIII. CONCLUSION

With the above experiments, that the concept of drive-by-wireless is feasible. Error detection is also made easier using this technique. Safety of the automobile system is also guaranteed. Complexity, bulkiness and heaviness of the system is reduced. The system is also made less expensive.

## REFERENCES

- [1] Hauke St'ahle, Kai Huang, Alois Knoll, "Drive-by-Wireless with the eCar Demonstrator", Proceedings of the 4th ACM SIGBED International Workshop on Design, Modeling, and Evaluation of Cyber-Physical Systems. ACM, pp. 1-4, 2014.
- [2] Mary, Gerardine Immaculate, Zachariah C. Alex, and Lawrence Jenkins., "REAL TIME ANALYSIS OF WIRELESS CONTROLLER AREA NETWORK.", ICTACT JOURNAL ON COMMUNICATION TECHNOLOGY, Volume.05, Issue. 03, pp.951-958, September 2014.
- [3] J.-R. Lin, T. Talty, and O. Tonguz, "Feasibility of safety applications based on intra-car wireless sensor networks: A case study", in Vehicular Technology Conference (VTC Fall), 2011 IEEE, pp. 1-5, 2011.
- [4] C. Buckl, A. Camek, G. Kainz, C. Simon, L. Mercep, H. Staehle, and A. Knoll, "The software car: Building ict architectures for future electric vehicles", in Electric Vehicle Conference (IEVC), 2012 IEEE International, pp. 1-8, March 2012.
- [5] M. Eder and A. Knoll, "Design of an experimental platform for an x-by-wire car with four-wheel steering", in Automation Science and Engineering (CASE), 2010 IEEE Conference on, pp. 656-661, 2010.
- [6] Lin, Jiun-Ren, Timothy Talty, and Ozan K. Tonguz, "An empirical performance study of Intra-vehicular Wireless Sensor Networks under WiFi and Bluetooth interference", In Global Communications Conference (GLOBECOM), 2013 IEEE, pp. 581-586, 2013.
- [7] Torbitt, C., Tomsic, K., Venkataraman, J., Tsouri, G. R., Laifenfeld, M., & Dziatczak, M., "Investigation of waveguide effects in intra-vehicular environments", In Antennas and Propagation Society International Symposium (APSURSI), pp. 599-600, July, 2014.
- [8] Ahmed, Mohiuddin, Cem U. Saraydar, Tamer ElBatt, Jijun Yin, Timothy Talty, and Michael Ames, "Intra-vehicular wireless networks", In Globecom Workshops, 2007 IEEE, pp. 1-9, 2007.
- [9] Lin, Jiun-Ren, Timothy Talty, and Ozan K. Tonguz. "On the potential of bluetooth low energy technology for vehicular applications." Communications Magazine, IEEE, Vol.53, Issue. 1, pp. 267-275, 2015.
- [10] Iturri, Peio Lopez, Erik Aguirre, Leire Azpilicueta, Uxue Garate, and Francisco Falcone, "ZigBee Radio Channel Analysis in a Complex Vehicular Environment [Wireless Corner]", Antennas and Propagation Magazine, IEEE, Vol.56, no. 4, pp.232-245, 2014.
- [11] Deng, Han, Jia Li, Liuqing Yang, and Timothy Talty, "Intra-vehicle UWB MIMO channel capacity", In Wireless Communications and Networking Conference Workshops (WCNCW), 2012 IEEE, pp. 393-397, 2012.
- [12] Lu, Ning, Nan Cheng, Ning Zhang, X. S. Shen, and Jon W. Mark, "Connected Vehicles: Solutions and Challenges", pp. 1-1, 2014.
- [13] Firmansyah, Eka, and Lafiona Grezelda, "RSSI based analysis of Bluetooth implementation for intra-car sensor monitoring", In Information Technology and Electrical Engineering (ICITEE), 2014 6th International Conference on, pp. 1-5, 2014.
- [14] Salahuddin, Mohammad A., Ala Al-Fuqaha, and Mohsen Guizan, "Software Defined Networking for RSU Clouds in support of The Internet of Vehicles", 2012.
- [15] Gerla, Mario, Eun-Kyu Lee, Giovanni Pau, and Uichin Lee, "Internet of vehicles: From intelligent grid to autonomous cars and vehicular clouds", InInternet of Things (WF-IoT), 2014 IEEE World Forum on, pp. 241-246. IEEE, 2014.



**Gerardine Immaculate Mary** received her M.Tech degree with specialization in Wireless Communication from Pondicherry Engineering College, Pondicherry. She is now Assistant Professor (Selection Grade), School of Electronics Engineering, Vellore Institute of Technology (VIT), Vellore.

She also has over 12 years of industrial experience as computer hardware engineer. Her research areas include wireless communication in automation and vehicular environments, indoor wireless positioning and Ultra Wide-Band Technology applications. She has published several research papers in international journals and conferences.



**S.Srinath** is currently studying final year B.Tech Electronic and Communication Engineering in VIT University, Vellore, India.



## International Journal of Innovative Research in Computer and Communication Engineering

(An ISO 3297: 2007 Certified Organization)

Vol. 2, Issue 6, June 2014

# Design of 4<sup>th</sup> Order Parallel Coupled Microstrip Bandpass Filter at Dual Frequencies of 1.8 GHz and 2.4 GHz for Wireless Application

S.Srinath

UG Student, Dept. Of ECE, Vellore Institute Of Technology, Vellore, Tamilnadu, India

**ABSTRACT:** Design of a parallel-coupled microstrip bandpass filter is presented in this paper. The aim of this paper is to present the design technique, parameter analysis, real prototype fabrication and measurement results at dual simulation frequencies of 1.8GHz and 2.4GHz. Half wavelength long resonators and admittance inverters are used to design the filter. The filter is simulated using AWR Microwave Office software (Advanced Wave Research).

**KEYWORDS:** Bandpass filter; Microstrip; 1.8 GHz & 2.4GHz; Parallel Coupled Line; Microwave Engineering; AWR Simulator.

### I.INTRODUCTION

The microwave filter is a two port network which used to control the frequency response by providing transmission at frequencies within the passband and attenuation in the stopband of a filter. Filters are an essential part of telecommunications and radar systems. Of its low-cost fabrication, easy integration and simple designing procedure, the parallel coupled-line/edge-coupled filters are widely used in microwave microstrip circuits with a required bandwidth up to 20 % of central frequency . A bandpass filter only passes the frequencies within a certain desired band and attenuates others signals whose frequencies are either below a lower cutoff frequency or above an upper cut-off frequency. The range of frequencies that a bandpass filter let's to pass through is referred as passband. A typical bandpass filter can be obtained by combining a low-pass filter and a high-pass filter or applying conventional low pass to bandpass transformation . The architecture demonstrated here is a coupled line type filter, since this is among the most practical and common filter types which can meet the stated specifications. In Coupled Transmission Lines, coupling between two transmission lines is introduced by their proximity to each other. Coupling effects may be undesirable, such as crosstalk in printed circuits, or they may be desirable, as in directional couplers where the objective is to transfer power from one line to the other . Another of their major use is using them in filtering the Microwave range frequencies.

The filter response will be based on the Chebychev transfer function. Chebychev type filters are popular for their high selectivity, i.e., they have a relatively fast signal cut off between pass and stop band. Filters operating in gigahertz frequency ranges rely on distributed transmission line structures to obtain the desired frequency response. Dimensions of the coupled transmission lines can be derived with published formula or minimal simulation software capability.

### II.RELATED WORK

This paper presents the design of a parallel-coupled microstrip bandpass. The design is based on the use of half wave long resonators and admittance inverters. The dual center frequencies of 1.8 GHz & 2.4GHz are selected, the bandwidth (BW) is about 5%, the minimum attenuation amounts to -30 dB and the pass-band ripple is obtained equal to 0.5 dB.The design technique, parameter analysis, real prototype fabrication and measurement results of a 4<sup>th</sup> order coupled line bandpass filter at a dual simulation frequencies of 1.8GHz & 2.4GHz is presented in this paper.

# International Journal of Innovative Research in Computer and Communication Engineering

(An ISO 3297: 2007 Certified Organization)

Vol. 2, Issue 6, June 2014

### III. THEORY

A general layout of a parallel coupled microstrip bandpass is shown in figure 3.1 . The filter structure consists of open circuited coupled microstrip lines . These coupled lines are quarter wavelength , ( $\lambda/4$ ) long and are equivalent to shunt resonant circuits. The coupling gaps correspond to the admittance inverters in the low-pass prototype circuit. Even- and odd- mode characteristic impedances of parallel-coupled half-wave resonators are computed using admittance inverters. These even- and odd- mode impedances are then used to compute physical dimensions of the filter. Now consider a bandpass filter composed of a cascade of  $N + 1$  coupled line sections, as shown in Figure 3.1. The sections are numbered from left to right, with the load on the right, but the filter can be reversed without affecting the response. Since each coupled line section has an equivalent circuit of the form, the equivalent circuit of the cascade is as shown in Figure 3.2.

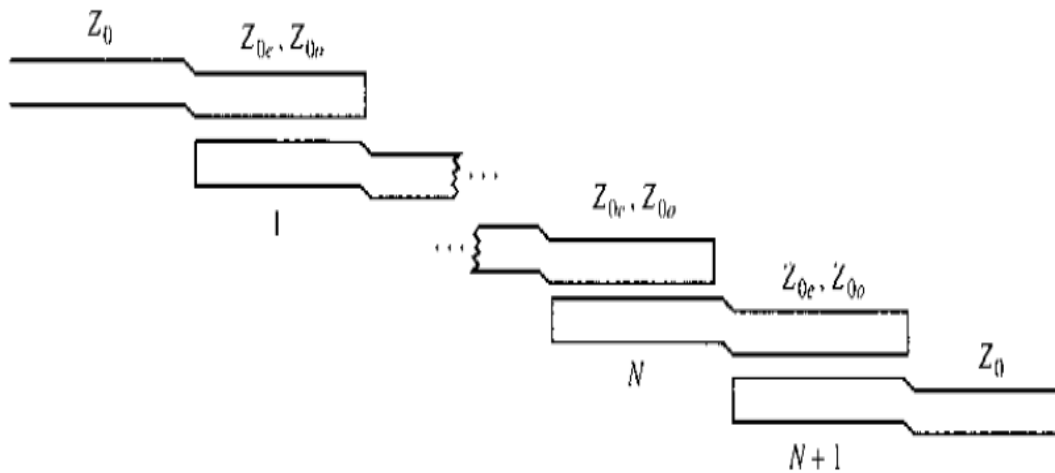


Figure 3.1 : Layout of an (N + 1)-section coupled line bandpass filter.

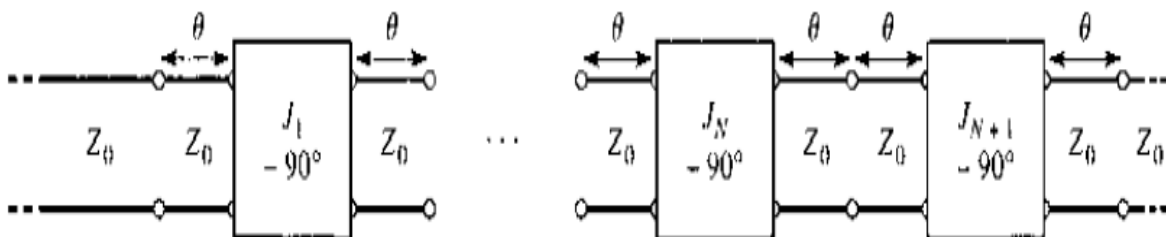


Figure 3.2 : Using the equivalent circuit of Figure 3.1 for each coupled line section.

# International Journal of Innovative Research in Computer and Communication Engineering

(An ISO 3297: 2007 Certified Organization)

Vol. 2, Issue 6, June 2014

## IV. IMMITANCE INVERTER

Immittance inverters play a very important role in filter design. They are used to transform a filter circuit into an equivalent form that can be easily implemented using various microwave structures. Immittance inverters are either impedance or admittance inverters. Making use of the properties of immittance inverters, bandpass filters may be realized by series (L-C) resonant circuits separated by impedance inverters (K) or shunt (L-C) parallel resonant circuits separated by admittance inverters (J). To design a bandpass filter, first of all a low-pass prototype circuit is modified to include immittance inverters. These low pass structures are then converted to bandpass circuits by applying conventional low-pass to bandpass transformation.

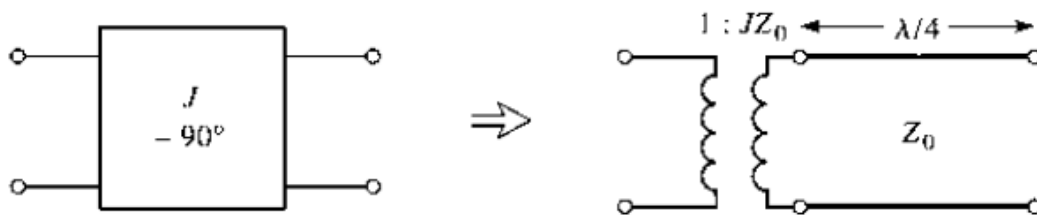


Figure 4.1 : Equivalent circuit of the admittance inverters.

## V.SIMULATION MODELING AND DISCUSSION

The design equations for the coupled line are as follows:

The order of the filter was calculated assuming an equi-ripple (Chebyshev type 1) response with an insertion loss (L) of 30dB at the center frequency of 1.8Ghz and 2.4Ghz and the passband ripple amplitude (G) of 0.5dB. The fractional bandwidth  $\Delta = 5\%$ .

Hence the upper and lower cutoff frequencies of the passband are 2.52 GHz and 2.28 GHz respectively. Using the standard Chebyshev model:

$$n = \frac{\cosh^{-1} \sqrt{(10^{\frac{L}{10}} - 1)/(10^{\frac{G}{10}} - 1)}}{\cosh^{-1}(\frac{f}{f_c})}$$

This gives us  $n = 4$ . Now, we get the lowpass prototype values from the standard Chebyshev table:

$g_0 = 1$
$g_1 = 1.6704$
$g_2 = 2.3662$
$g_3 = 0.8419$
$g_4 = 1.9841$
$g_5 = 1.6704$

Now, we use the following design equations to get the inverter constants for a coupled line filter with  $N+1$  sections:

$$Z_0 J_1 = \frac{\sqrt{\Pi \Delta}}{\sqrt{2g_1}}$$

$$Z_0 J_n = \frac{\Pi \Delta}{2\sqrt{g_{n-1} g_n}} \quad ; n = 2, 3, 4 \dots N$$

# International Journal of Innovative Research in Computer and Communication Engineering

(An ISO 3297: 2007 Certified Organization)

Vol. 2, Issue 6, June 2014

$$Z_0 J_{n+1} = \sqrt{\frac{\Delta \Pi}{2g_n g_{n+1}}}$$

Using these equations, we get:

$Z_0 J_1 = 0.2168$
$Z_0 J_2 = 0.0556$
$Z_0 J_3 = 0.0467$
$Z_0 J_4 = 0.0556$
$Z_0 J_5 = 0.2168$

Now, the even and odd mode impedances can be calculated as follows:

$$Z_{oe} = Z_0 [1 + JZ_0 + (JZ_0)^2]$$

$$Z_{oo} = Z_0 [1 - JZ_0 + (JZ_0)^2]$$

The results of these calculations are tabulated below:

N	$Z_{oe}(\Omega)$	$Z_{oo}(\Omega)$
1	63.191	41.512
2	52.934	47.378
3	52.446	47.778
4	52.936	47.377
5	63.192	41.514

The substrate used is a standard FR4 substrate (MSUB) with  $\epsilon_r = 4.4$ ,  $H = 1.58\text{mm}$ ,  $T = 0.036\text{mm}$  and  $T_{and} = 0.005$ . Using a coupled line calculator, the width, length and line spacing for each coupled line was calculated:

Line	W(mm)	L(mm)	S(mm)
1	2.70182	69.11613	0.794745
2	2.98623	68.10692	3.450721
3	3.0021	68.05937	3.948424
4	2.98624	68.10694	3.450725
5	2.70188	69.11616	0.794743

Based on the above values and taking standard port impedances as  $Z_0 = 50\Omega$ , the design was simulated.

# International Journal of Innovative Research in Computer and Communication Engineering

(An ISO 3297: 2007 Certified Organization)

Vol. 2, Issue 6, June 2014

## V.SIMULATION DESIGN, RESULTS & DISCUSSION

The design was simulated using AWR Design Environment (9.00.4847) and a response was generated. The coupled line design used for simulation was MCFIL which is a non-floating line. This is a coupled line model with the end effect included for the open ended line. One side of each coupled line is the ground plane.

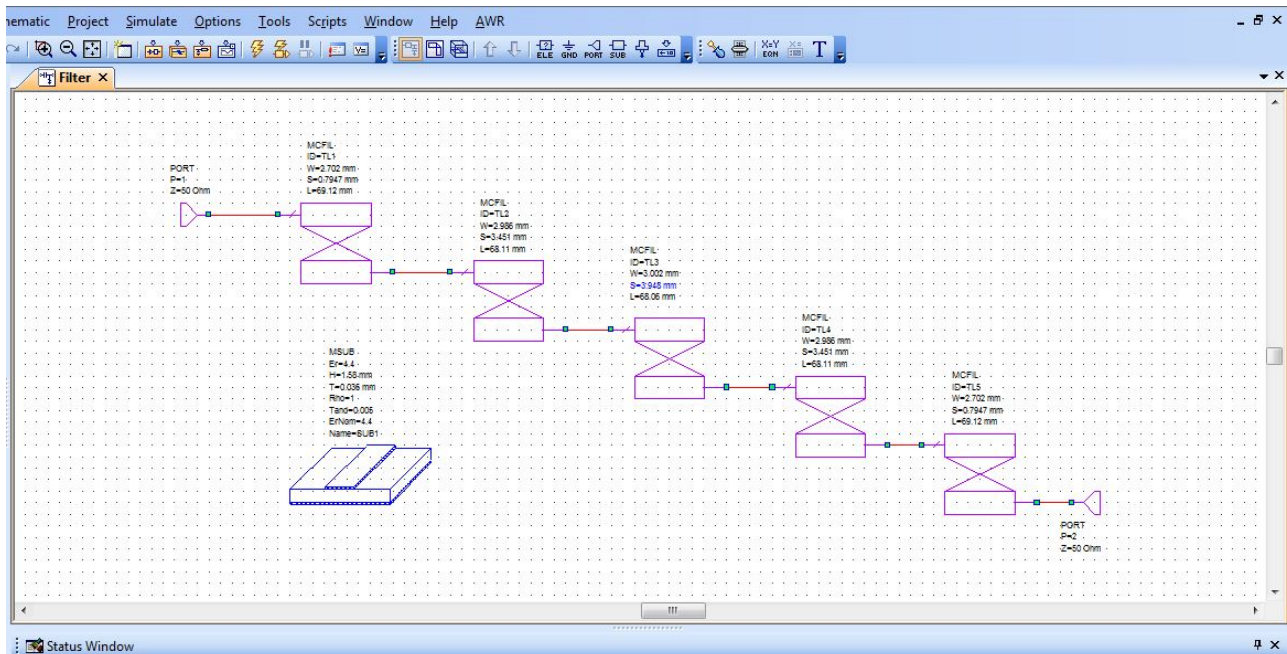


Figure 5.1 : Layout of the proposed 4<sup>th</sup> order filter design in AWR Software

Here, the parameter  $S_{11}$  (dB) represents the insertion loss at port 1 and this parameter which has a value of -6.521dB at the center frequency of 2.4 GHz while -6.587dB at the center frequency of 1.8GHz

The parameter  $S_{21}$  (dB) represents the insertion loss from port 1 to port 2 which has a value of -2.633dB at the center frequency of 2.4GHz while -6.375dB at the center frequency of 1.8GHz.

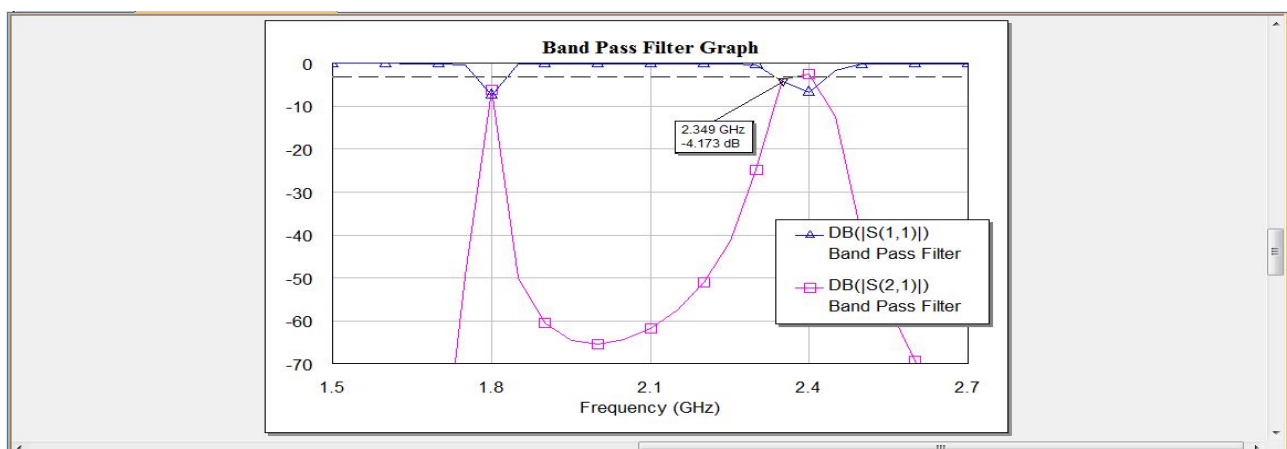


Figure 5.2 : Coupled Line Bandpass Filter at Dual Frequencies Result

The first design discussed above was simulated in AWR. The same was simulated using EM simulation. The schematic diagram for the same is given below:

# International Journal of Innovative Research in Computer and Communication Engineering

(An ISO 3297: 2007 Certified Organization)

Vol. 2, Issue 6, June 2014

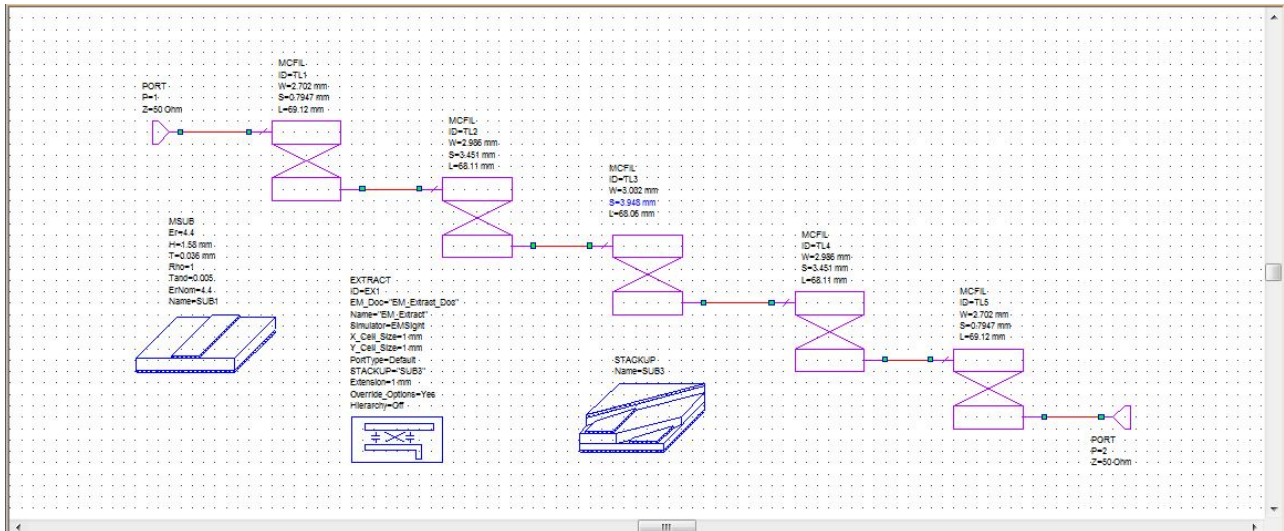


Figure 5.3 : Layout of the proposed 4<sup>th</sup> order filter design in AWR Software using EM simulation

Here, the parameter  $S_{11}$  (dB) represents the insertion loss at port 1 and the parameter which has a value of -2.606dB at the center frequency of 2.4 and 1.8GHz

The parameter  $S_{21}$  (dB) represents the insertion loss from port 1 to port 2 which has a value of -16.87dB at the center frequency of 2.4GHz while -31.55dB at the center frequency of 1.8GHz.

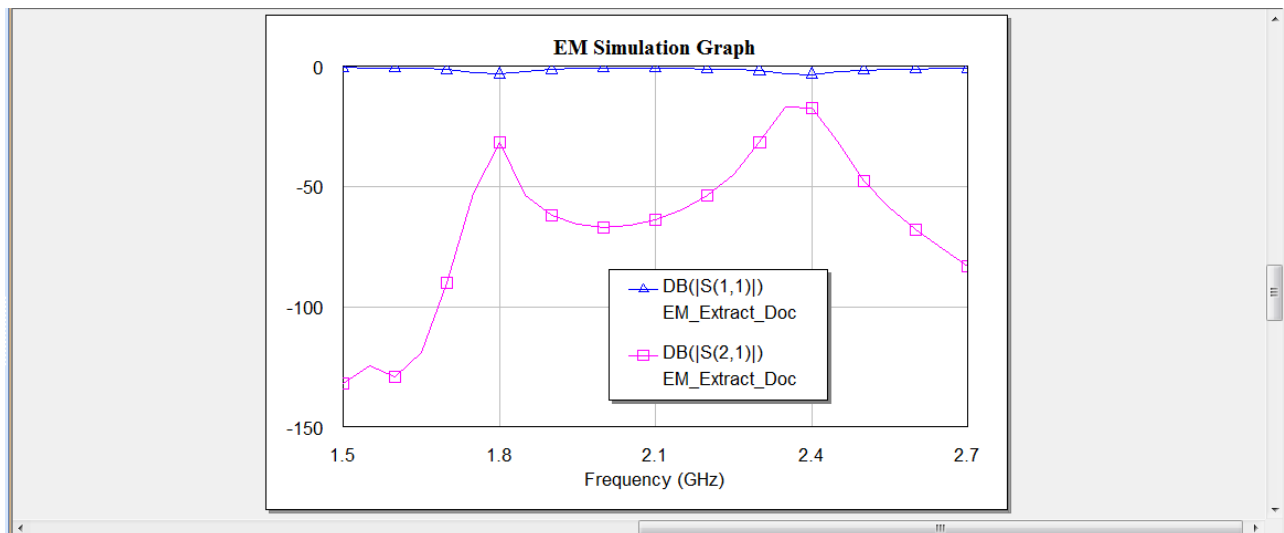


Figure 5.4 : Coupled Line Bandpass Filter at Dual Frequencies EM Simulation Result

For the Stackup, the dielectric used is FR4 and the conductor is copper. The transmission lines used in the design are MCLIN which are essentially similar to MCFIL lines with their remaining ends left open. The thickness of the dielectric layer is taken as 1.58mm and air thickness is taken as 24mm.

The simulation is done on EMSight with X and Y cell resolution of 0.5mm and an extension of 1mm. The extracted EM schematic is given below:

# International Journal of Innovative Research in Computer and Communication Engineering

(An ISO 3297: 2007 Certified Organization)

Vol. 2, Issue 6, June 2014

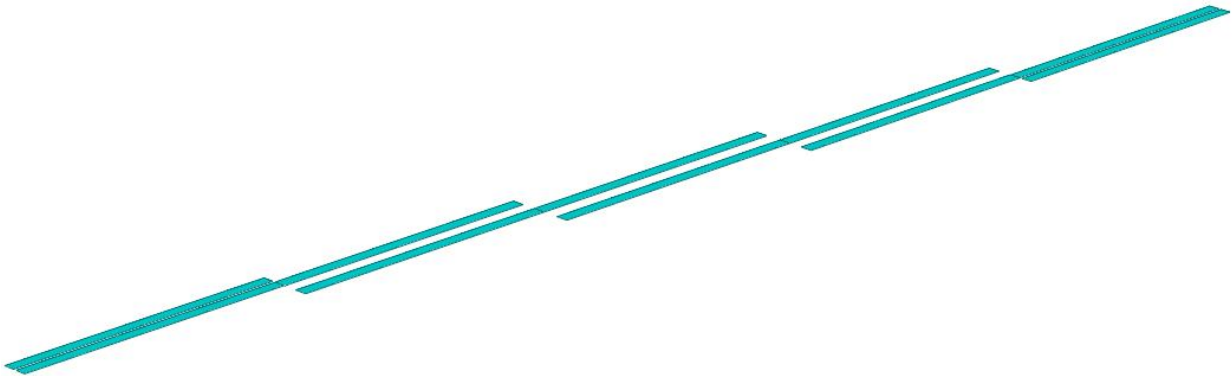


Figure 5.5 :3D View of the Coupled Line Bandpass Filter

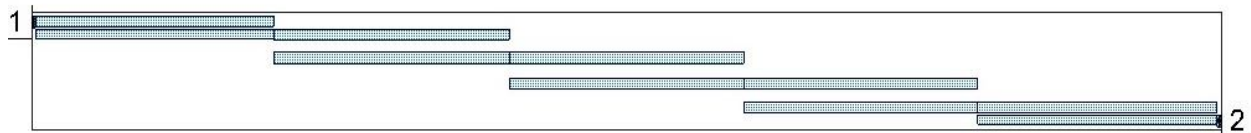


Figure 5.6 :3D View of the Extraced EM Strucure

## VI.CONCLUSION

On a substrate with a dielectric constant of 4.4, with the dual center frequencies of 1.8 GHz & 2.4 GHz, a coupled line bandpass filter was simulated with the bandwidth of about 5%, with the minimum attenuation of 30 dB and with the pass-band ripple equal to 0.5 dB. Thus the design technique, parameter analysis, real prototype fabrication and measurement results at dual simulation frequencies of 1.8GHz and 2.4GHz of a 4th order coupled line bandpass filter was presented in this paper.

## VIII.ACKNOWLEDGEMENT

At the outset, I would like to express my gratitude for my institute – Vellore Institute of Technology (V.I.T.) for providing me with the opportunity to undergo my undergraduate training, and assimilate knowledge and experience hitherto unknown to me.



# International Journal of Innovative Research in Computer and Communication Engineering

(An ISO 3297: 2007 Certified Organization)

Vol. 2, Issue 6, June 2014

## REFERENCES

- [1] D. M. Pozar, "Microwave Engineering", John Wiley & Sons Inc., 1998.
- [2] Miguel Bacaicoa, David Benito, Maria J. Garde, Mario Sorolla and Marco Guglielmi, "New Microstrip Wiggly-Line Filters with Spurious Pass-band Suppression", IEEE Transactions on microwave theory and techniques, vol. 49, no. 9, September 2001.
- [3] John T. Taylor and Qiuting Huang, "CRC Handbook of Electrical Filters", CRC Press, pp. 22-23, 1997.
- [4] "Tuning, Optimization and Statistical Design", Agilent Technologies, May 2003.  
R. Levy, S. B. Cohn, "A History of Microwave Filter Research, Design, and Development", Microwave Theory and Techniques, IEEE Transactions, vol. 32, no. 9, pp. 1055,1067, Sep 1984.
- [5] A. Naghar, O. Aghzout, F. Medina, M. Alaydrus, M. Essaidi, "Study and Design of a Compact Parallel Coupled Microstrip Band-Pass Filter for a 5 GHz Unlicensed Mobile WiMAX Networks," International Journal of Science and Technology, vol. 2, No. 6, June 2013.  
Sina Akhtarzard, Thomas R. Rowbotham, and Petter B. Johns, "The Design of Coupled Microstrip Lines", IEEE Transactions on Microwave Theory and Techniques, vol. MTT-23, no. 6, pp. 486-492, June 1975.  
E. O. Hammerstad, "Equations for microstrip circuit design," in Proceedings of the European Microwave Conference, Hamburg, Germany, 1975, pp. 268–272.
- [6] Annapurna Das and Sisir K Das, "Microwave Engineering", MacGraw Hill, p305, 2001.
- [7] Hong, J.S., M.J, "Microstrip Filter for RF/Microwave Applications", A Wiley- Interscience Publication, Canada, 2001.
- [8] C. A Balanis, "Antenna Theory: Analysis and Design", 3rd edition, Wiley, 2005.
- [9] S. B. Cohn, "Parallel-Coupled Transmission-Line-Resonator Filters," Microwave Theory and Techniques, IRE Transactions on , vol. 6, no. 2, pp. 223-231, April 1958.
- [10] S. Seghier, N. Benahmed, F. T. Bendimerad, N. Benabdallah, "Design of parallel coupled microstrip bandpass filter for FM Wireless applications", Sciences of Electronics, Technologies of Information and Telecommunications (SETIT), 6th International Conference , pp.207-211, 21-24 March 2012.  
A. R Othman, I.M. Ibrahim, M. F. M. Selamat, M. S. A. S. Samingan, A. A. A. Aziz, H. C. Halim, "5.75 GHz microstrip bandpass filter for ISM band", Applied Electromagnetics, APACE Asia-Pacific Conference on , pp. 1-5, 4-6 Dec. 2007.  
I. Azad, Md. A. H. Bhuiyan, S. M. Y. Mahbub, "Design and Performance Analysis of 2.45 GHz Microwave Bandpass Filter with Reduced Harmonics", International Journal of Engineering Research and Development, vol. 5, no. 11, pp. 57-67, 2013.
- [11] John T. Taylor and Qiuting Huang, "CRC Handbook of Electrical Filters", CRC Press, pp. 22-23, 1997.

## BIOGRAPHY



**S.SRINATH** passed 10<sup>th</sup> C.B.S.E. Board with a mark of 475/500(95%) and 12<sup>th</sup> C.B.S.E. Board from D.A.V. Boys Senior Secondary School, Gopalpuram, Chennai with a mark of 458/500(91.6%). Currently he is studying B.Tech, ECE, School of Electronics Engineering in VIT University, Vellore, India.

# Design and Real Prototype Fabrication Of a Free Space Optical Transmitter and Receiver

S.Srinath

UG Student, ECE, Vellore Institute of Technology, Vellore, India

**Abstract:** We are communicating with each others for every purpose. Different modes of communication are used. Free space optics is one of the mode of communication. Free space optics is widely used by satellites for transmitting with each other. Design and real prototype fabrication of a low cost portable free space optical transmitter and receiver is presented in this paper. Using this prototype wireless communication is possible. Light from a laser torch is used as the carrier in the circuit. The laser torch can transmit light up to a distance of about 500 meters. The transmitter circuit comprises of condenser microphone transistor amplifier BC548. The gain of the op-amp can be controlled with the help of 1-mega-ohm potmeter. The transmitter uses 9V power supply. The receiver circuit uses an npn phototransistor as the light sensor that is followed by a two-stage transistor preamplifier and LM386-based audio Power amplifier. This paper deals with the designing of a very low cost free space optical system which is perfect for information transmission of general conversation, using an ordinary available Laser torch of cost. The circuit is designed using National Instrumentations Multisim11.0 (**N.I. Multisim 11.0**) and National Instrumentations UltiBoard11.0 (**N.I. UltiBoard 11.0**).

**Keywords:** Battery driven design, Free space optics, Laser torch, Low cost design, N.I. Multisim and N.I. UltiBoard Simulator, Voice or data transmission.

## I. INTRODUCTION

This paper is based on the concept of Laser (Light Amplification by Stimulated Emission of Radiation) for transmitting analog as well as digital signals. As laser is stimulated radiation, problem of interference occurs in electromagnetic wave is eliminated, it can be a good substitution of present day communication systems and high deal of secrecy is available. Use of laser in communication systems is the future because of the advantages of the full channel speeds, no communication licenses required at present, compatibility with copper or fiber interfaces and no bridge or router requirements. Also it cannot be detected with use of spectrum analyzers and RF meters and hence can be used for diverse applications including financial, medical and military. Lasers can also transmit through glass. Laser transmitter and receiver units ensure easy, straightforward systems alignment and long-term stable, service free operation, especially in inaccessible environments. Optical wireless systems offer ideal, economical alternative to expensive leased lines for buildings. The laser can be commissioned in satellites for communication, as laser radar requires small aperture as compared to microwave radar. For voice transmission amplitude modulation of laser pulse was used to transmit the voice signal. Condenser microphone converts the voice into electric pulse which was then amplified and transmitted through laser. Photo detector at receiver detects the laser light and voice was output through loud speaker.

## II. RELATED WORK

This paper presents the design and real prototype fabrication of a free space optical system. The circuits are simulated in N.I. Multisim 11.0 and checked for validity and routing for the P.C.B. design is done with N.I. UltiBoard 11.0. The given design is thus checked and

routed as per 'INDUSTRY STANDARDS' and the real prototype can thus be etched out and a P.C.B. can be made on which components can be easily soldered. This paper mainly focuses on checking the validity of my design and performing a routing for my design for making a P.C.B.

## III. OBJECTIVES OF THE DESIGN

This paper aims to provide simple and cheap wireless communication design and real prototype fabrication for larger data rate with less distortion and to reduce the complexity for communication in the places where optical fiber or any wired communication is very difficult and expensive. The design is so easy, inexpensive and makeable with the available equipments that the technical as well as non technical person can construct it by themselves for their personal use.

### A. Block Diagram and Algorithm used for the Design

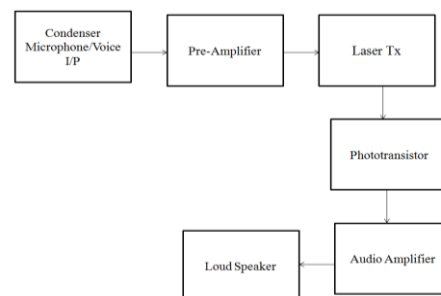
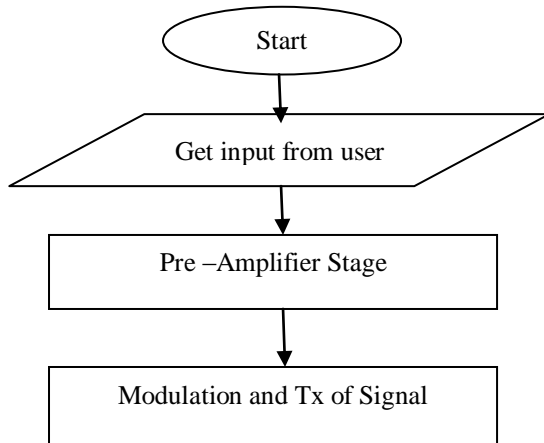


Fig. 1 Block Diagram for Voice and Data Transmission

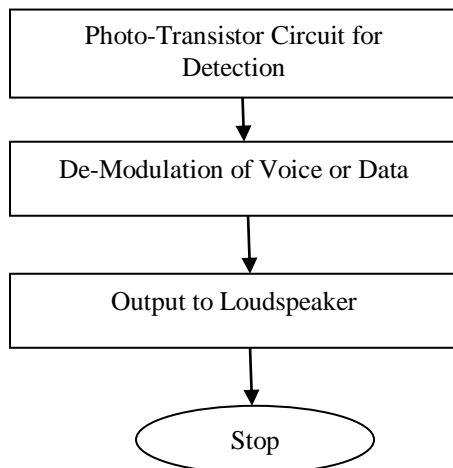
The algorithm is as follows. The input voice is taken through condenser microphone or a plug-in is taken as the input. The voice signal is amplified through the

preamplifier phase. Then, the signal is transmitted through laser light. The phototransistor at receiving side converts the signal into electrical signal. The electrical signal is passed through two transistor amplifier phases. Then LM386 audio amplifier amplifies the signal and drive speaker to generate voice output.

Flow Chart for Transmitter Circuit :



Flow Chart for Receiver Circuit :



#### IV. EQUIPMENTS REQUIRED

TABLE I  
EQUIPMENTS REQUIRED

Resistors All of (1/4)W, 5% unless otherwise stated	Capacitors	Others
10R (brown, black, black) 1 Num	100 uF electrolytic 1Num	LM 358 IC 2Nos
100R (brown, black, brown) 2 Num.	10 uF electrolytic 3Nos.	LM 386 IC 1Num.
1K (brown, black, red) 1Num	100 nF monoblock (104) 4 Nos.	78L05 regulator 1Num

10K (brown, black, orange) 1Num	10 nF mylar (103) 2 Nos.	BC547 transistor 1 Num.
22K (red, red, orange) 2 Nos.	47nF box poly 1 Num	IF-D93 detector (red dot on black case) 1Num
100K (brown, black, yellow) 4Nos	-	IF-E96 emitter (pink dot on blue case) 1Num
220K (red, red, yellow) 1 Num.	-	Electret Microphone 1Num
680K (blue, grey, yellow) 1Num.	-	Speaker 8 ohm, 1W 1Num
1M (brown, black, green) 1Num.	-	8 pin DIL IC socket 3 Nos.
100K Koa trimpot (104) 1Num.	-	2 pole terminal block 3Nos.
-	-	9V battery snap 2Nos.

#### V. WORKING OF CIRCUIT DIAGRAM OF TRANSMITTER

The electret microphone converts sound waves to an electrical signal in the Tx circuit. R1 provides DC bias for the microphone and should be removed if you wish to connect any other input instead. This signal is coupled via C2 and amplified by two LM358 op amps, and converted to an optical signal by the LED emitter, driven from transistor Q1. R3 and R6 set the gain of IC1A to 1+R3/R6, or 221. Since IC1A is direct coupled, R4/R2 determine the DC input and thus the DC output level. IC1B is also direct coupled and provides both the DC base current for Q1 and the AC modulation current. R7 determines the DC bias current for Q1. The modulated collector current drives the LED emitter.

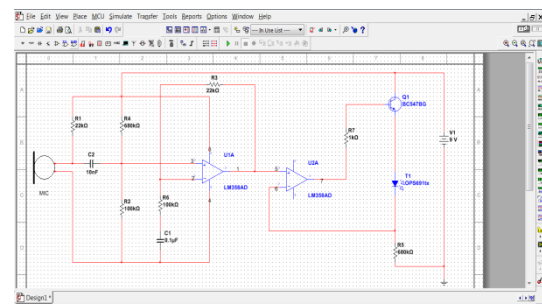


Fig. 2 Transmitter schematic in N.I. Multisim 11.0

#### VI. REAL PROTOTYPE FABRICATION OF TRANSMITTER

After checking the validity of the circuit in N.I. Multisim11.0, now convert the circuit to UltiBoard 11.0. To do this check if all the components are blue in colour(i.e. they have a foot-print) and select 'Transfer To UltiBoard 11.0' button.

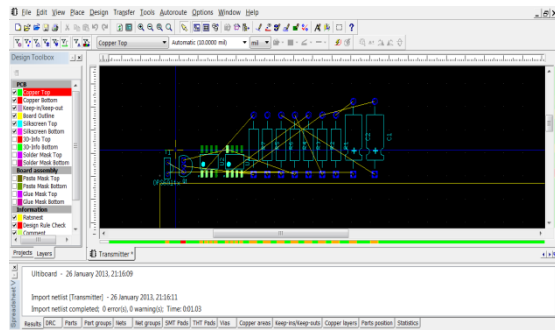


Fig. 3 Basic View of the Converted Schematic in N.I. UltiBoard 11.0

Now, align the components on the workspace and perform 'Routing'.

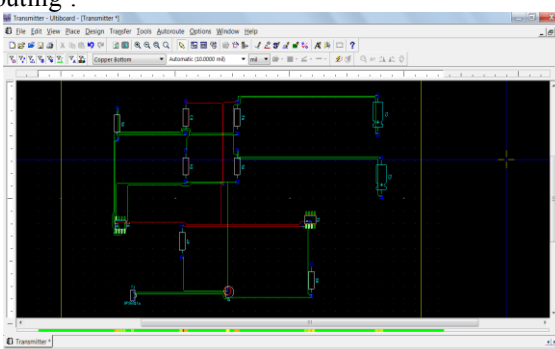


Fig. 4 View after Performing Routing of the Schematic in N.I. UltiBoard 11.0 for Transmitter Design

The 3D View of the real prototype fabrication of my design is shown below.



Fig. 5 3D View of my Design Showing PCB Connections for Transmitter Design



Fig. 6 3D View Showing Connections Appearing at the back-side of the PCB for Transmitter Design

## VII. WORKING OF CIRCUIT DIAGRAM OF RECEIVER

At the other end of the cable, the optical signal is directed at a photo-darlington detector in the receiver that converts it into an electrical signal again. The signal is amplified by op amp IC2 and power amp IC3 before being fed into a speaker where it becomes a sound wave. A voltage regulator has been used in the receiver gain stage to reduce DC supply ripple caused by the higher currents drawn in the power amplifier section. C1 and C2 are filter caps, C3 couples the detector voltage imposed across R1, into IC2. R2 and R4 set the op amp input to half the supply voltage, since only one supply is used rather than positive and negative supplies, as is usually the case. The gain of IC2 is adjustable by the pot in the feedback circuit. The range is therefore 1+1M/110k to 1+1M/10k, or 10 to 101. This is used as a volume control. IC2 output is coupled via C6 into an LM386 power amp IC with gain set to 20. R6 and C8 act as a low pass filter on the input. R7 and C9 form a network that provides a high frequency load to ensure stability.

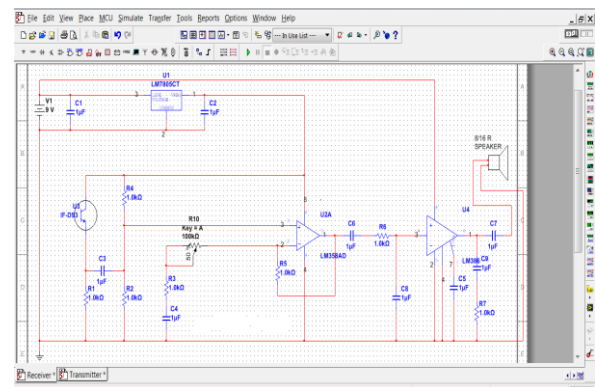


Fig. 7 Receiver schematic in N.I. Multisim 11.0

## VIII. REAL PROTOTYPE FABRICATION OF RECEIVER

After checking the validity of the circuit in N.I. Multisim11.0, now convert the circuit to UltiBoard 11.0. To do this check if all the components are blue in colour(i.e. they have a foot-print) and select 'Transfer To UltiBoard 11.0' button.

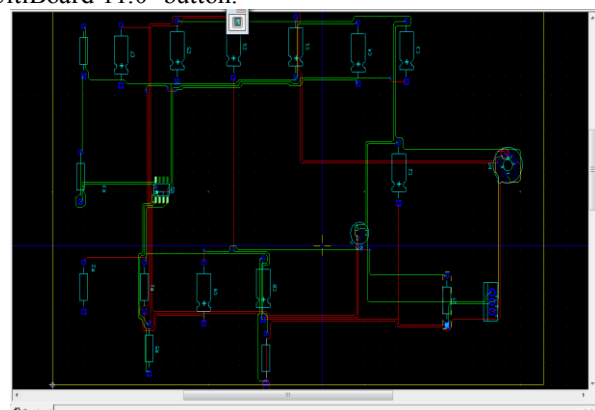


Fig. 8 View after Performing Routing of the Schematic in N.I. UltiBoard 11.0 for Receiver Design

The 3D View of the real prototype fabrication of my design is shown below.

## Thank You for previewing this eBook

You can read the full version of this eBook in different formats:

- HTML (Free /Available to everyone)
- PDF / TXT (Available to V.I.P. members. Free Standard members can access up to 5 PDF/TXT eBooks per month each month)
- Epub & Mobipocket (Exclusive to V.I.P. members)

To download this full book, simply select the format you desire below

